Band-resolved analysis of nonlinear optical properties of crystalline and molecular materials

Ming-Hsien Lee, Chou-Hsun Yang, and Jeng-Huei Jan
Department of Physics, Tamkang University, Tamsui, Taipei 251, Taiwan
(Received 22 October 2003; revised manuscript received 7 September 2004; published 7 December 2004)

Through three case studies, plane wave pseudopotential density functional theory calculations are performed to investigate the mechanism of second harmonic generation (SHG) of the nonlinear optical materials. We want to know how SHG coefficients are affected by: (1) anion substitution in $AgGa(S_xSe_{1-x})_2$; (2) the isomeric effect in push-pull benzenes; and (3) the length of π-conjugate chain in push-pull polyenes. A sum-over-states type formalism is used for the evaluation of static SHG coefficients. Orbital contribution to the β or $\chi^{(2)}$ can be decomposed on a (energy) level-by-level basis by partially summing only two out of all three band indices. Through such process that we proposed, the dominant orbitals that give major contribution to a SHG process can then be identified and analyzed. These so-called "band-resolved" plots of SHG coefficient are sensitive to the variation of structure and configuration of the materials, and can thus be used to study the detailed mechanism of SHG processes in crystals and molecules.

DOI: 10.1103/PhysRevB.70.235110 PACS number(s): 71.15.Dx, 78.20.Bh, 42.65.Ky, 42.70.Mp

I. INTRODUCTION

The practical (nondivergent) formalism for evaluating nonlinear optical (NLO) properties for solids was proposed by Sipe *et al.*[1,2] and further rearranged by Rashkeev.[27] Apart from the remarkable breakthrough of making calculation possible, the use of such a sum-over-states formalism has the advantage of providing a natural way to see the total quantities as contribution from various parts. For example, the optical quantities are expressed in terms of wave functions (momentum matrix elements) and eigenvalues with band indices, it is possible to decompose them by either partitioning wave functions or just selectively summing a subset of indices of energy levels. Complicated solids or molecules can have many components contributing to their overall optical properties. To understand the mechanism in terms of these partial or local contributions, a strategy for "local analysis" is essential and we will propose one in this work. Case studies for both crystalline solids and molecules will be used to demonstrate the advantage of such scheme for understanding the mechanism of second harmonic generation (SHG) of the materials.

The first case study will be on chalcopyrite $AgGa(S,Se)_2$. Both $AgGaS_2$ and $AgGaSe_2$ are important infrared (IR) NLO crystals.[3–5] In addition to the second-order susceptibility, $\chi^{(2)}$, which characterizes the optical nonlinearity of a crystal and determines the conversion rate of SHG process, band gap and IR absorption edge are two quantities of particular importance for application. A wider band gap allows higher power pumping for the production of visible SHG beam. A lower IR absorption edge/threshold leaves a broader transparent range, so that injected IR beam will not be absorbed by the crystal itself. Among these two crystals, $AgGaS_2$ has the advantage of having a wider band gap, but its IR absorption edge/threshold is higher and also its $\chi^{(2)}$ is smaller. On the contrary, $AgGaSe_2$ has the advantage of having lower IR absorption edge/threshold and larger $\chi^{(2)}$ than $AgGaS_2$, but its band gap is smaller. It is therefore very desirable to mix-grow these two crystals so that optimal properties for a specific application can be obtained. The tuning of the mechanical property, IR absorption edge, and band gap of the crystalline material through forming a solid solution of $AgGaS_2$ and $AgGaSe_2$ will be discussed elsewhere.[6,7] In this work we concentrate only on the mechanism of how $\chi^{(2)}$ changes according to the anion-substitution in $AgGa(S_xSe_{1-x})_2$, and how our analysis methods help to find the answer.

The second and third case studies will be on push-pull polyene and benzene. The idea of using a longer conjugate chain in order to achieve a larger first-order and second-order hyperpolarizability was proposed a long time ago.[8] A polyene oligomer is such a conjugate system, which is also a perfect one-dimensional model for theoretical study.[9–15] This type of molecule probably has the largest first-order hyperpolarizability (β) ever reported.[10,11] The material produces a strong electro-optic (Pokels) effect and therefore has the potential application in devices such as modulators and switches. Benzene is an important building block in organic molecules. Its planar six-member ring helps to establish a strong intermolecular interaction crucial for forming molecular crystals. Many organic NLO crystals contain this building block. One of the simplest configurations of push-pull benzenes is nitroaniline (NA), which has three structural isomers. Understanding the underlying mechanism of how SHG varies between these isomers may provide an useful insight for the molecular design of both organic and inorganic NLO materials.[16] There have been extended theoretical studies on these organic NLO molecules.[17–24] However, in the present work we intend to use a density functional theory (DFT) plane wave pseudopotential computational scheme, which is usually adapted in studying solid-state and surface problems. This methodology will allow us to work on larger (or even periodic) systems in the future, such as NLO molecules on surface and NLO properties of exotic nanostructures.

In the following sections, the method of calculation and the approach of analysis will be given in Sec. II. In Sec. III, we report the results of our case studies starting from $AgGa(S_xSe_{1-x})_2$, which are three-dimensional semiconductor

crystals. It is then followed by the results of isomers of planar molecules nitroaniline, and finally that of typical one-dimensional push-pull polyenes $H_2N\text{-}(CH{=}CH_2)_n\text{-}NH_2$. The conclusion will be drawn in Sec. IV.

II. METHODOLOGY

CASTEP,[25] a planewave pseudopotential code based on the DFT, is used to carry out the electronic structure calculations. Norm-conserving optimized pseudopotentials generated by one of the authors are used.[26] In the case of $AgGaS_2/AgGaSe_2$, a plane wave energy cutoff $E_{cut}=500$ eV is enough to converge the ground state energy of a system to be smaller than 0.1 eV per atom compared to the case when an extremely high plane wave energy cutoff is chosen. SHG coefficients are not very sensitive to the E_{cut} anymore if the planewave basis set of this quality or higher is used. The spacing of *k*-point sampling grid for the semiconductor crystals was chosen to be around 0.1 $Å^{-1}$ for electronic structure minimization and 0.05 $Å^{-1}$ for optical matrix element calculations. We have compared the three-electron Ga pseudopotential with a 13-electron one to see whether the ten *d* electrons in the semicore is important in our case. The results turn out to be that the interested optical properties of $AgGaS_2$ and $AgGaSe_2$ are already reproducible using the three-electron Ga pseudopotential. The three-electron one is therefore used throughout the study. In the cases of push-pull benzene and polyene, a big supercell is used to properly simulate a molecule in vacuum (the size of the supercell box is chosen to ensure there is more than 8 Å vacuum between each periodic image), also $E_{cut}=600$ eV is used because the carbon potentials require higher E_{cut} to converge. To calculate optical properties, a larger number of unoccupied bands is needed. Throughout this work, twice the total number of valence bands is used, which is verified by convergence tests to be sufficient for the purpose of this study.

To evaluate the SHG coefficients, we have adapted the formalism proposed by Rashkeev[27] and later improved by Lin.[28] This sum-over-states type formalism is explicitly expressed with terms having momentum matrix elements in numerator and energy eigenvalue difference in denominator. In the present work, the entire SHG coefficient of a molecule (β) or a crystal [$\chi^{(2)}$] are divided into contribution from virtual hole (VH), virtual electron (VE), and two-band processes, as what we have done in the study of NLO oxide crystals.[28–31] The contribution from two-band process is extremely small and can be neglected. Furthermore, by partially summing only two out of all three band indices, the value of SHG strength was decomposed into two representations of orbital contributions, namely occupied and unoccupied bands, based on two different types of summing sequences. A plot of the band-resolved SHG coefficient, as we call it, can thus be obtained, which gives the orbital contribution of the β or $\chi^{(2)}$ in a (energy) level-by-level basis. Through such process, the dominant orbitals giving major contribution to a SHG process can be identified and later analyzed. Given the SHG strength of individual orbital revealed, it can be used to study the effect on SHG due to structural or configurational change in a material. Moreover,

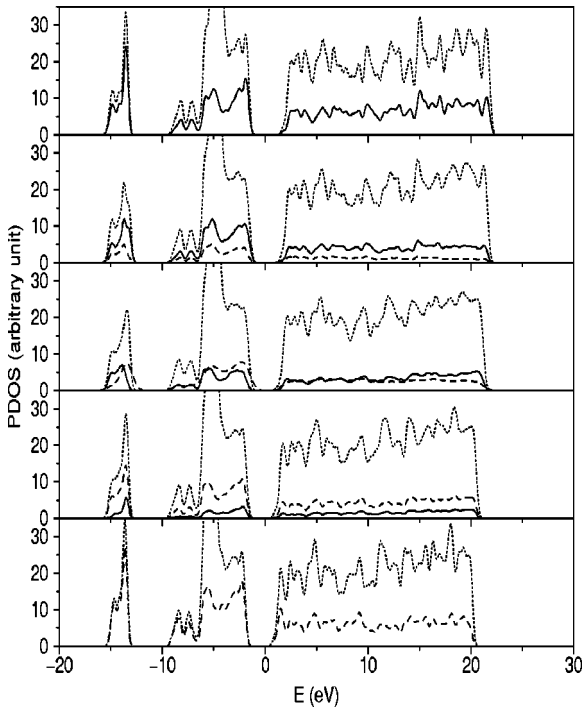

FIG. 1. PDOS of $AgGa(S_xSe_{1-x})_2$, from top to bottom $x=1.0$, 0.75, 0.5, 0.25, and 0.0. Solid lines are the S contribution, dashed lines are Se contribution and dotted lines are total DOS. One can see that the S and Se show a similar PDOS plot among different anion substitution ratios, this indicates that these two types of anions play the same role in terms of their local energy levels. In other words, they are chemically similar.

re-evaluating $\chi^{(2)}$ or β using artificially adjusted eigenvalue spectra helps to determine the role played by the energy level of orbitals.

Not only resolving the contribution through bands, we have also performed the so-called real-space atom-cutting analysis[28] which is based on partitioning the wave function of a local collection of atoms and evaluate their partial contribution to β. This method is particularly useful in the case of molecules.

It is known that within the framework of the Kohn-Sham DFT scheme, band gap correction of some kind, such as the so-called scissors correction, may be required for predicting linear and nonlinear optical properties more accurately. However, as will be shown from the results of this work, the trend of SHG coefficients calculated without band gap correction already agrees well with what are measured experimentally. The Kohn-Sham gap is therefore used throughout this work.

III. CASE STUDIES AND RESULTS

A. $AgGa(S_xSe_{1-x})_2$

The most obvious difference between $AgGaS_2$ and $AgGaSe_2$ crystals is their anions. We want to know how the difference of anion species affects the $\chi^{(2)}$ of the crystals. Five plots of the projected density of states (PDOS) of crystals with [S]:[S+Se] ratio ranging from 100%, 75%, 50%, 25% to 0% is shown in Fig. 1, each cell contains 64 atoms

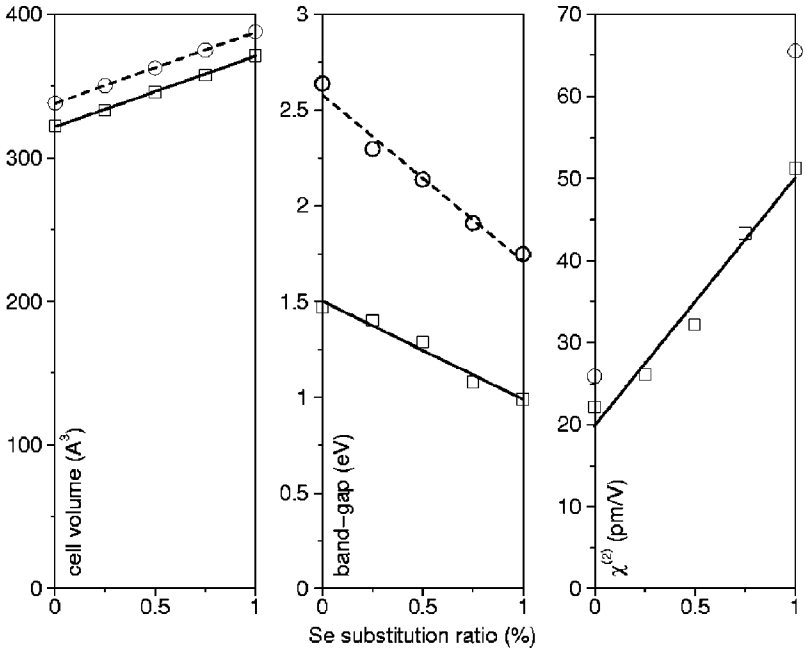

FIG. 2. Calculated properties of $AgGa(S_xSe_{1-x})_2$ (square marks) compared with experimental values[6] (circle marks). Lines are linear fits of data. Left panel: cell volume (in Å^3) vs Se ratio $1-x$. Middle panel: DFT band gap (in eV) vs Se ratio $1-x$. Right panel: $\chi^{(2)}$ (in pm/V) vs Se ratio $1-x$. They all show a linear trend with respect to the concentration of Se. The correlation between cell volume, band gap, and $\chi^{(2)}$ suggests that the variation of $\chi^{(2)}$ might be a volume effect.

with anions positioned randomly. This suggests that S and Se are remarkably similar in terms of their chemical behavior, they (locally) sit at the same energy region in the crystals. Given the $\chi^{(2)}$ variation is not caused by the chemical nature of the two group-VI elements, one may turn to seek for some more "physical" reasons. Figure 2 shows how the substitution ratio affects the cell volume, band gap and $\chi^{(2)}$, respectively. Clearly, there is a correlation between the volume, band gap, and $\chi^{(2)}$, which suggests the variation of $\chi^{(2)}$ and band gap may simply be a volume effect.

In order to know whether this band gap and $\chi^{(2)}$ variation is purely a volume effect, we have designed a computer experiment based on varying the volume of unsubstituted $AgGaS_2$ and $AgGaSe_2$ cells and observed how the band gap and $\chi^{(2)}$ change. For $AgGaS_2$, we change its volume gradually to that of $AgGaSe_2$, which is a 15% increase equivalent to a 5% linear expansion. Similarly, the volume of the $AgGaSe_2$ cell is compressed to become that of $AgGaS_2$. The result, Fig. 3, shows that such volume expansion alone is sufficient to reproduce the kind of variations in band gap and $\chi^{(2)}$ observed in anion-substituted crystals. The observed correlation between volume and $\chi^{(2)}$ as well as volume and band gap is therefore not an accident. Furthermore, when the same gap value is assumed artificially to evaluate the $\chi^{(2)}$ of crystals with various volume, the slope of $\chi^{(2)}$ becomes much flatter than it should be, as shown in Fig. 4. This indicates that the $\chi^{(2)}$ variation is largely controlled by the band gap. A simple picture of the mechanism can therefore be established as the cell volume controls the band gap which finally affects the value of $\chi^{(2)}$.

On the other hand, from the viewpoint of sum-over-states formalism, the contribution to $\chi^{(2)}$ can be regarded as coming from two sources, namely the momentum matrix elements in the numerators and the energy level differences in the denominators. The level-by-level (band-by-band) decomposition of $\chi^{(2)}$, as shown in Fig. 5 and using the $AgGaS_2$ case as

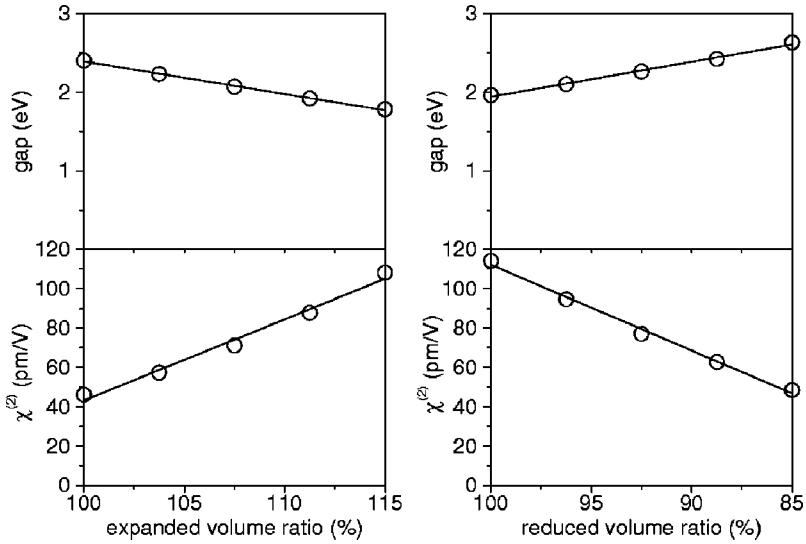

FIG. 3. The trend of calculated band gap and $\chi^{(2)}$ (marks) due to the expansion and compression of pure crystals $AgGaS_2$ (left panel) and $AgGaSe_2$ (right panel). Lines are linear fits. The change of cell volume is sufficient to reproduce the linear change of band gap and $\chi^{(2)}$.

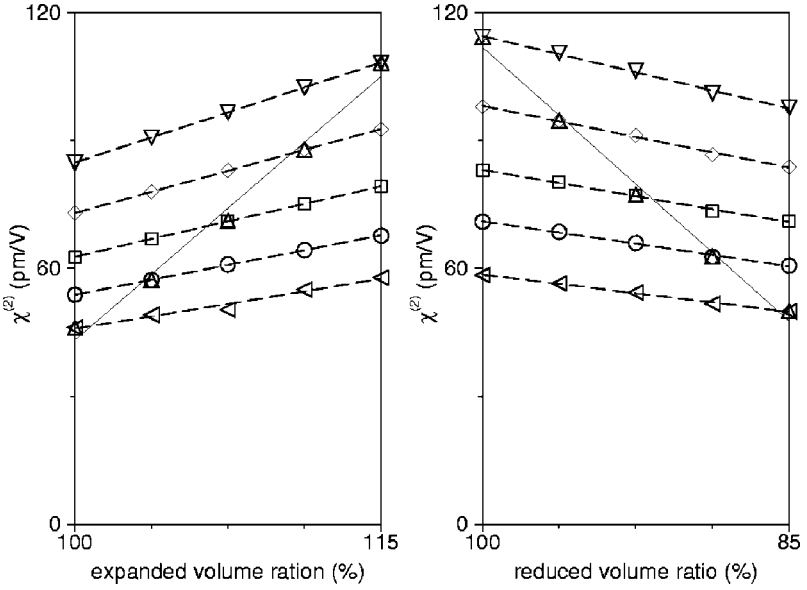

FIG. 4. Original (solid lines) and "equal-gap" re-evaluated (dashed lines) $\chi^{(2)}$ of $AgGaS_2$ (left panel) and $AgGaSe_2$ (right panel). For those five cell volumes marked with the same symbol (dashed line), their band gaps are adjusted to be identical for evaluating $\chi^{(2)}$. Significant reduction of the slope indicates that the band gap has to play an important role in $\chi^{(2)}$ variation, while the reminding slope suggests the existence of other factor(s).

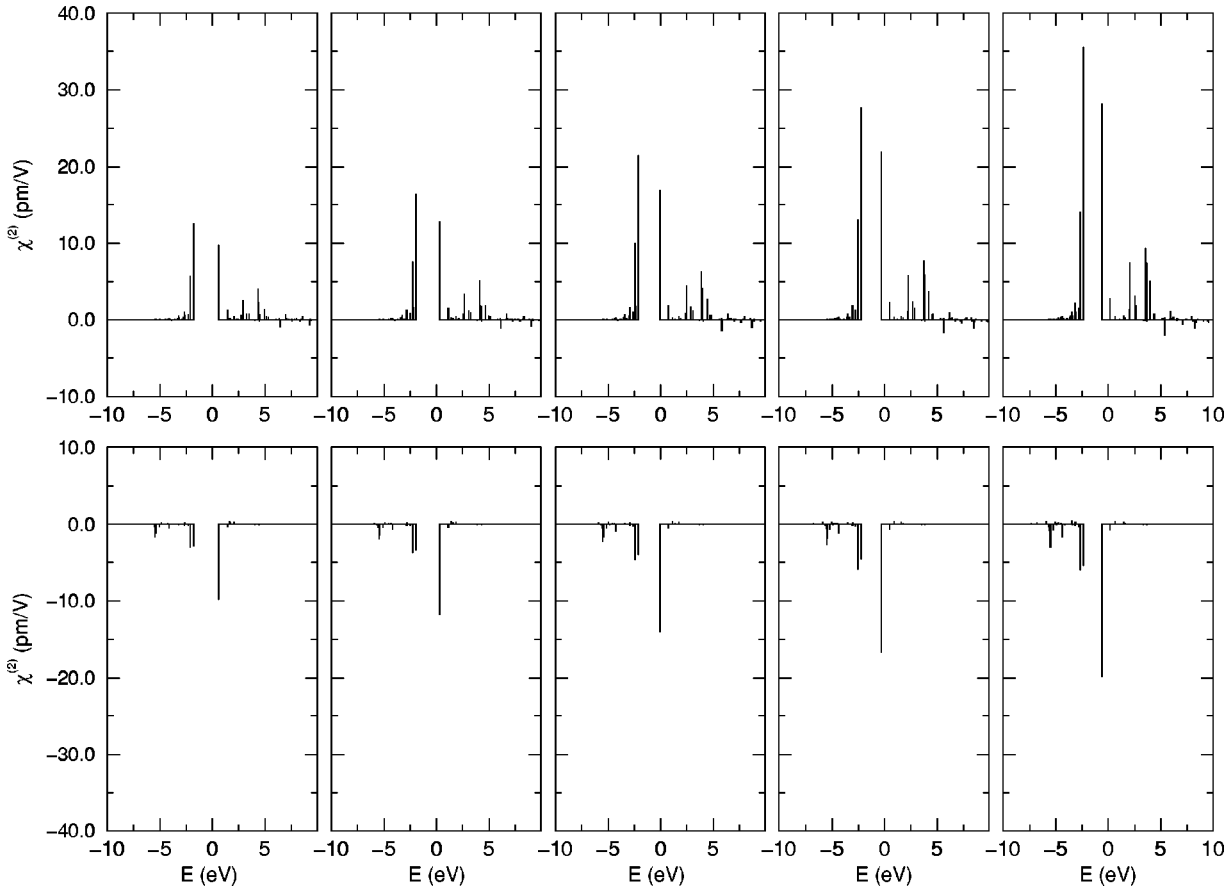

FIG. 5. Band-resolved $\chi^{(2)}$ of $AgGaS_2$ at zone center. The upper row are the virtual electron contributions and the lower row are the virtual hole ones. The five cell volumes are displayed from left to right, corresponding to the uniform expansion from 100% to 115%. One can see that these "densities of $\chi^{(2)}$" share the same pattern, also the energy level spacing reduces with respect to the increase of cell volume. (Note that in each plot, summing up all the peaks on the left to the band gap will get same value as summing up all the peaks to the right, which is equal to the $\chi^{(2)}$ of that process.) In this material, the virtual electron process is more important than virtual hole processes, and they are in opposite directions so they have a cancellation effect. Other *k* points show the same behavior but the magnitude is smaller. The results of $AgGaSe_2$ are similar to those of $AgGaS_2$ and are therefore not shown here.

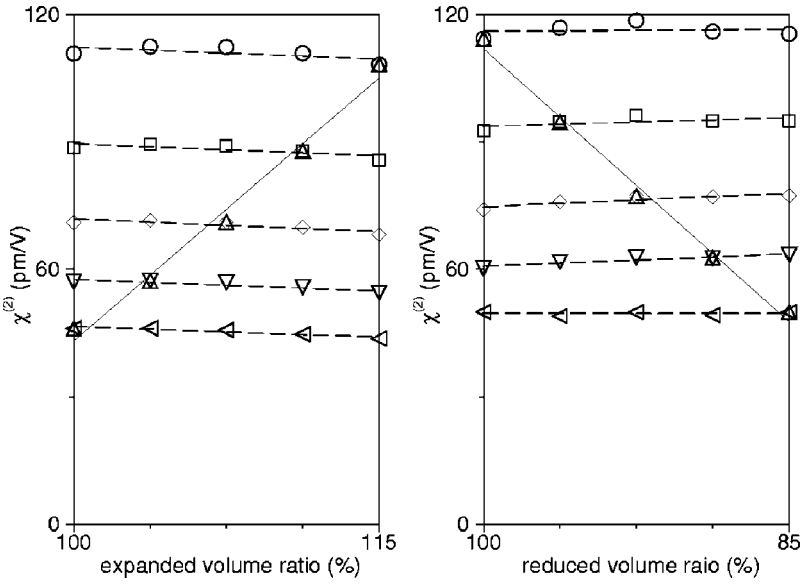

FIG. 6. The original $\chi^{(2)}$, of $AgGaS_2$ (left panel) and $AgGaSe_2$ (right panel), are shown alone fitted solid lines, while the fitted dashed lines emphasize the re-evaluated $\chi^{(2)}$ of those crystals with different cell volumes but using the same energy level spacing from only one of the crystals. One can see that these dashed line are much flatter than the original solid lines. This indicates the effect of energy level spectra solely controls the $\chi^{(2)}$ in these crystals.

an example, does indeed reveal the trend of level spacing becoming smaller when the cell volume increases. (Incidentally, the k points near the zone center make a larger contribution than those that are not.) If the entire energy level spectrum (i.e., band structure) from one cell is used for cells with different volumes, these cells still give almost the same $\chi^{(2)}$ even though their volumes are different, as shown in Fig. 6. Note that the wave functions, and therefore the matrix elements, of those crystals remain in their original values. This result indicates that the energy level spacing that appears in the denominator of the $\chi^{(2)}$ formula plays the exclusively dominant role in the determination of the $\chi^{(2)}$ variation of the anion-substituted $AgGaS_2/AgGaSe_2$ system. We believe this can be understood through a simple "particle in a box" picture, where energy level spacing becomes narrower when the box size becomes bigger. Therefore, the mechanism of the $\chi^{(2)}$ variation due to the anion S:Se substitution can be understood as the following: different anion size causes the crystals to pack into different volume, which in turn makes the spacing of the energy levels different and finally results in a different $\chi^{(2)}$. In simple terms, this is purely a volume effect.

B. Para-, meta-, and ortho-push-pull benzene (nitroaniline: *p*NA, *m*NA, *o*NA)

The structural isomers of nitroaniline, a push-pull benzene, exhibit three distinctive geometric forms. They therefore allow one to study how their hyperpolarizability (β) is affected by the relative geometrical arrangements of push (NH_2) and pull (NO_2) functional groups. The orientation of these molecules in supercells is arranged in such a way that their largest β are pointing to the z axis, as shown in Fig. 7. The calculated and measured values of β are shown in Table I. Our results reproduce not only the trend of β measured experimentally,[32] which is $p\text{NA} > o\text{NA} > m\text{NA}$, but also their order of magnitude. The convergence of β with respect to the number of unoccupied orbitals is shown in Fig. 8. This suggests that only a fairly small number of unoccupied bands is needed.

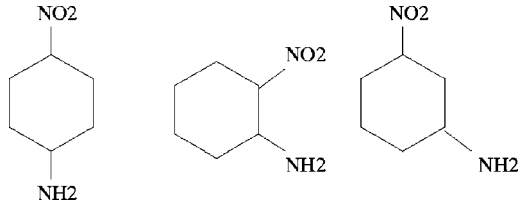

FIG. 7. The structure of *p*NA (left), *o*NA (center), and *m*NA (right). The orientation of these molecules has been chosen so that the direction of their largest β is pointing upwards.

Band-resolved β in Fig. 9 shows a significant difference between the VE and VH processes. We found that the VH process contributes more or less the same to the molecular hyperpolarizability, especially for the case of *p*NA and *o*NA. While for the VE process, the contributions vary from fairly large, dominating the β of *p*NA, to medium, comparable with the VH contribution in *o*NA, then to very small in the case of *m*NA. For *p*NA, the VE process is about a factor of 3 more important than the VH process, and for *o*NA, the contribution of VE reduced to two thirds of VH. As for *m*NA, one can see the cancellation of two occupied orbitals taking place resulting in a very small contribution to the z direction (the largest β direction). The molecular geometry of the isomers obviously has much more effect on the VE process than on the VH process.

It is natural to ask whether it is again the energy spectrum controlling the SHG coefficients, as in the case of $AgGaS_2/AgGaSe_2$. Although the ordering of the energy ei-

TABLE I. β (in 10^{-30} esu) of the three isomers of NA.

Isomer	Calc.	Expt.[a]
*p*NA	47.4	34.5
*o*NA	23.9	10.3
*m*NA	7.5	6.0

[a]Reference 32.

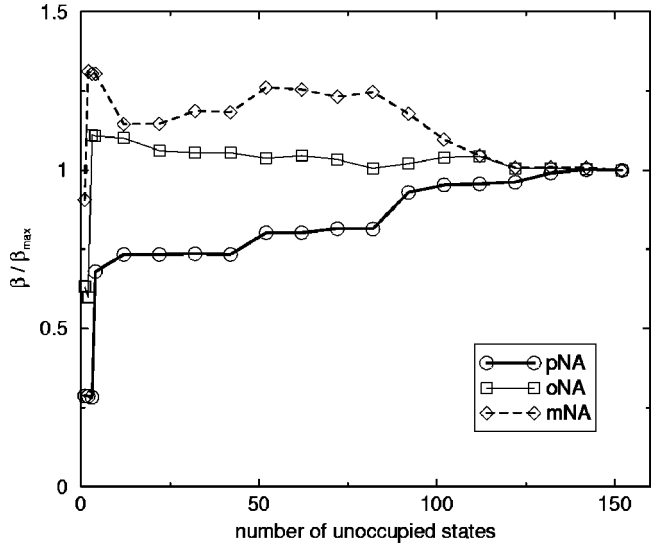

FIG. 8. Convergence tests of β with respect to the number of unoccupied states used, for three NA isomers. The β calculated using 150 unoccupied bands, which corresponding to twice the number of occupied bands, are designated as $\beta_{\max}$. The plots show the ratio of $\beta/\beta_{\max}$ when each particular number of unoccupied bands is used.

genvalues may not be the same among isomers, this does not cause any complication when we want to artificially change the energy levels of (important) orbitals and to re-evaluate β. The five most important orbitals (three occupied, two unoccupied) in Fig. 9 are all in the same spectral order and have the same characteristics among isomers, as verified by examining their wave functions. Most of the triple products of momentum matrix elements between bands, which appear as numerators in the formula of β, are far too small compared with those very few from the important bands. In fact we have compared the value of β recalculated using two methods, either by completely neglecting unimportant orbitals or by uniformly scaling their energies between two adjusted important orbitals, the results are indeed not distinguishable. This confirms that in this particular case, it is sufficient to deal with only the important orbitals identified by band-resolved analysis (Fig. 9), and to adjust the energy levels of those few states, which obviously have the right symmetry to maximize the triple products of momentum matrix elements. The result, shown in Table II, indicates that the trend of β is controlled not by the energy level spectra, but by the matrix elements of isomers. It is also important to see, from Table III, that the ratio due to the change of spectra is insensitive to whichever matrix element set is used, and likewise the ratio due to the change of the matrix element is insensitive to whichever eigenvalue specta are used. This suggests that these two effects are disentangled and can somehow be factored out and understood as two independent contributions to the hyperpolarizability of the molecules.

TABLE II. Energy level replacement for push-pull benzene. The values are re-evaluated β (in 10^{-30} esu), for example, the value corresponding to $M(p\text{NA})$ and $E(m\text{NA})$ means using the energy level spacing of important orbitals from *m*NA and using the momentum matrix element from *p*NA. The values on the diagonal are the original ones. One can see that it is the matrix elements that determine the trend of the β.

	$E(p\text{NA})$	$E(o\text{NA})$	$E(m\text{NA})$
$M(p\text{NA})$	47.40	93.55	61.24
$M(o\text{NA})$	11.68	23.90	15.66
$M(m\text{NA})$	5.40	9.71	7.45

It is also important to observe that only several major eigenstates are involved, typically two or three from each side near the highest occupied molecular orbital (HOMO)/lowest unoccupied molecular orbital (LUMO) gap. However,

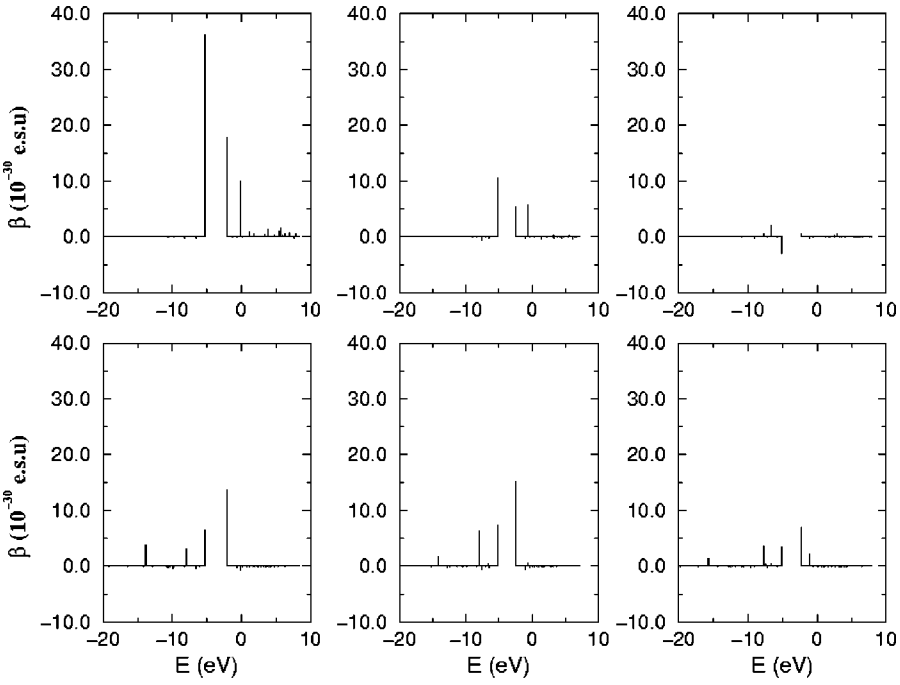

FIG. 9. The band-resolved β of three geometrical isomers of NA. From left to right are *p*NA, *o*NA, and *m*NA, respectively. Both VE contribution (upper panels) and VH contribution (lower panels) are shown. One can see a larger variation coming from VE processes rather than VH ones.

TABLE III. The top and bottom tables show how β change (in terms of ratio) due to the change of energy level spacing and matrix element sets, respectively. For example, the value corresponding to $E(p\text{NA}\rightarrow o\text{NA})$ means the ratio of β changes due to the replacement of energy levels of *p*NA by those of *o*NA while using the same set of matrix elements. One can see the remarkably similar ratio in both tables.

	$E(p\text{NA}\rightarrow o\text{NA})$	$E(o\text{NA}\rightarrow m\text{NA})$	
$M(p\text{NA})$	1.97	0.65	
$M(o\text{NA})$	2.05	0.66	
$M(m\text{NA})$	1.80	0.76	
	$E(p\text{NA})$	$E(o\text{NA})$	$E(m\text{NA})$
$M(p\text{NA}\rightarrow o\text{NA})$	0.25	0.26	0.26
$M(o\text{NA}\rightarrow m\text{NA})$	0.46	0.41	0.48

this also suggests that the hyperpolarizability could be poorly approximated within a two-level model, at least for a quantitative prediction, as often seen in the literature. One can also see that all these important orbitals to β have π-symmetry, with no exception. The usual understanding is that the poor overlap between atomic "p_z" orbitals makes the bonding/antibonding energy splitting of π-orbitals significantly smaller than that of orbitals with σ-symmetry, making π-orbitals nearest to the HOMO/LUMO gap and give the largest contribution to β because of their appearance as small energy denominators.

We found that those important orbitals (SHG-MO) can be classified into two categories, namely push-derived and pull-derived. For example, HOMO orbitals are push-group (NH_2) derived and LUMO ones are pull-group (NO_2) derived. This can easily be identified by observing the nodal plane structure driven by different orientation of respective functional groups, as shown in Fig. 10. The classification allows one to understand why the order of β is $\beta(p\text{NA})>\beta(o\text{NA})>\beta(m\text{NA})$. In particular, the results of $\beta(o\text{NA})>\beta(m\text{NA})$ do not seem to be expected using an intuitive

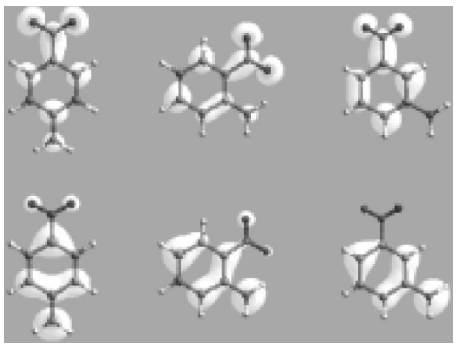

FIG. 10. HOMO (bottom row) and LUMO (top row) orbital densities of three isomers of NA. From their nodal structure one can clearly see the HOMO orbitals being derived from push group (NH_2) and the LUMO ones from pull group (NO_2). One can also see that the overlap between push-derived and pull-derived MO are strongest in the case of *p*NA (left), moderate in *o*NA (center), and weakest in *m*NA (right).

TABLE IV. The partial contribution to β (in 10^{-30} esu) from different molecular fragments of NA is listed for its three isomers. The additivity errors between the total sums and the original full values are also given.

	NH_2	C_6H_4	NO_2	Total sum	Original	Additivity (%)
*p*NA	12.39	29.97	12.47	54.83	47.70	15.68
*o*NA	3.06	13.96	8.24	25.26	23.90	5.96
*m*NA	1.74	5.92	1.17	8.83	7.45	18.52

"dipole model" where the size of β is proportional to the dipole moment of the molecule: since *m*NA has larger expand of push and pull groups than *o*NA, a dipole model would have predicted $\beta(m\text{NA})>\beta(o\text{NA})$. We observed very strong hybridization between push- and pull-derived SHG-MO in the case of *p*NA, while in *o*NA such effect is moderate. As for *m*NA, its push-derived and pull-derived states do not mix at all. When evaluating momentum matrix elements, the well-delocalized states of *p*NA therefore have big "on-site" transition because of the good overlap of wave functions, making the β of *p*NA the largest. The same argument also applies when explaining why $\beta(o\text{NA})>\beta(m\text{NA})$. The β is therefore, in this manner, affected by the molecular geometry/topology. In fact, chemists have interpreted this unexpected trend of β of NA isomers in terms of whether it is possible to have "resonance form" for these various isomers.[33,34] The difference in the degrees of delocalization of SHG-MO observed in this work, which is likely due to the symmetry of the nodal structure of wave functions determined by molecular frameworks, supports the resonance form interpretation.

Complementing the band-resolved scheme, Table IV shows the partial contribution to β due to different molecular fragments of the isomers, analyzed using the atom-cutting approach.[28] The largest contribution comes from the benzene ring, which is typically more than half of the total β. The additivity is good for the way the system is partitioned. With the error only around 10%, the validity of the methodology is justified.

C. Push-pull polyenes

It is well known that the hyperpolarizability of push-pull polyenes increases dramatically with respect to the length of their π-conjugated chain, at least for the cases where the chain length is not too long. How the length of such molecules affecting their β is a subject of interest. We calculated the β of NH_2-$(C_2H_2)_n$-NO_2 and list the results in Table V, which does show such a trend. A convergence test of β has already been carried out to ensure the number of unoccupied

TABLE V. Calculated β for push-pull polyenes with different length.

n	1	2	3	4	5
β (10^{-30} esu)	7.74	42.14	168.64	421.44	917.27

TABLE VI. The ratio of β increase with respect to the chain length.

$n \rightarrow n+1$	LDA[a]	GGA[a]	TDHF[b]	MP2[b]	HF[b]
$1 \rightarrow 2$	5.5	5.2	4.9	4.2	4.8
$2 \rightarrow 3$	4.0	3.8	2.9	2.7	2.7
$3 \rightarrow 4$	2.5	2.5	2.2	2.0	2.0
$4 \rightarrow 5$	2.2	2.2	1.8	1.7	1.6

[a]Current work, in which PW91 (Ref. 36) is the version of GGA used.
[b]Reference 20, notations used here are as defined in the original paper.

orbitals used is sufficient. Results from current work are also compared with those from other quantum chemistry methods, as shown in Table VI. It is known that the β of push-pull polyene calculated using the DFT method tends to increase more significantly with respect to the increase of chain length.[35] This is also seen in the current work.

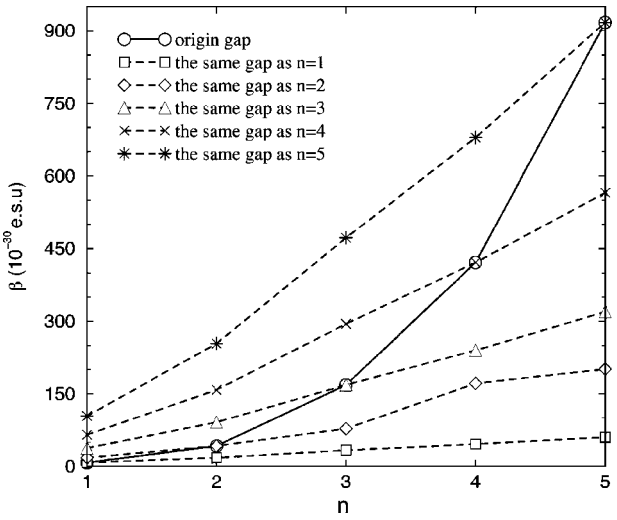

FIG. 11. Re-evaluated β (in 10^{-30} esu) for polyenes of different length using the same HOMO/LUMO gap values.

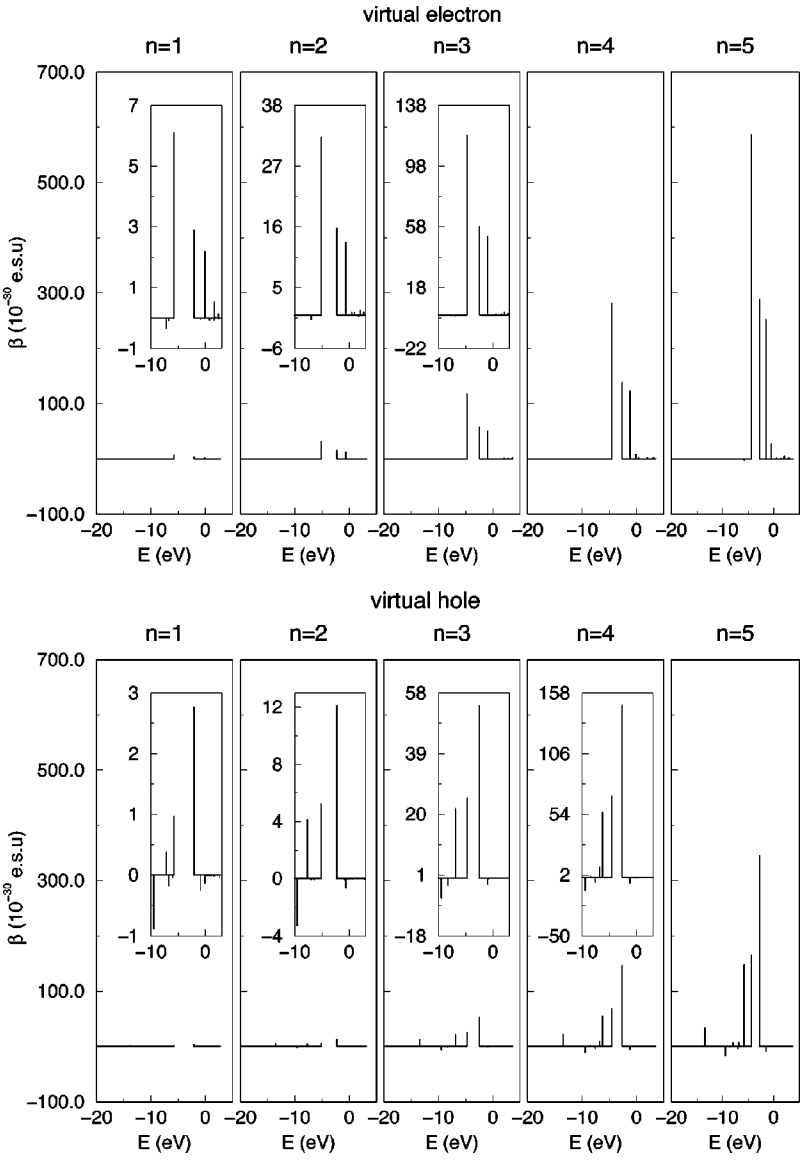

FIG. 12. Band-resolved β of polyenes from $n=1$ (left) to $n=5$ (right). The added little frames in each case are the same plots magnified accordingly for easy inspection. One can see the pattern is similar throughout the plots, and the energy level spacing decreases with respect to n, i.e., the length of the molecules.

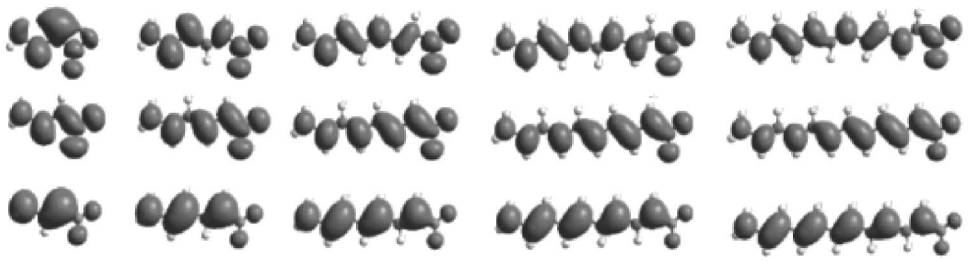

FIG. 13. Electron density of molecular orbitals that contribute large hyperpolarizibility as picked-up by band-resolved SHG plots Fig. (12). Cases with molecular length $n=1-5$ are arranged from left to right; for each molecules, their most important orbitals, HOMO, LUMO, LUMO$+1\pi$, are arranged from bottom to top.

For these polyene molecules, a quick and simple re-evaluation of β using a same HOMO-LUMO gap does not result in any significant change, as shown in Fig. 11. The trend of their β therefore has little to do with the gaps of the molecules.

As in the previous case of nitroaniline, band-resolving β analysis is used to analyze the β of push-pull polyene. We found, as shown in Fig. 12, the β from the VE processes are typically a factor of 1.5–2 to the VH ones, and in the same sign. It is very important to note that although these push-pull polyene molecules come in different lengths, the key orbitals that contribute the β (i.e., SHG-MO) are very similar and are in fact of equivalent characteristics (see Fig. 13) and line up in the same (spectral) order. This is a great advantage of our band-resolved analysis over the applied field (derivative) techniques, as it would be impossible to reveal the important SHG-MO if the latter were used. Using a "full band structure" method, we are able to truly identify important MO instead of making assumptions, such as in the case of the two-level model. As expected, all of these orbitals are again π-orbitals.

Although the energy level indices are very different for molecules at different lengths, only the few SHG-MO identified by the band-resolved method are needed for performing spectrum replacement. The energy level and matrix element effects on hyperpolarizibility can thus be obtained by re-evaluation of β, as shown in Table VII. It reveals that the energy level spacing is the most important effect. Whenever n increase by one unit (i.e., two carbon atoms), that effect magnifies the β by 2–3.5 times, depending on the original chain length. Although the matrix element plays some part in molecules of $n=1$ and $n=2$, the effect saturates for $n>2$.

TABLE VII. This table shows the β (10^{-30} esu) of push-pull polyenes $NH_2(C_2H_2)_nNO_2$. $M(n)$ means using the matrix element of molecule with n C_2H_2 pairs, while $E(n)$ means using the eigenvalue spectrum from molecule with n C_2H_2 pairs. The following two tables show the ratio of how β change aroding to the change of energy level spacing or matrix element sets, respectively. Whichever matrix elements set is used, it is not sensitive to the change of energy level spacing. Such results suggest one can divide the contribution of β into two independent factors.

β	$E(1)$	$E(2)$	$E(3)$	$E(4)$	$E(5)$
$M(1)$	7.74	26.18	80.45	183.09	372.05
$M(2)$	12.18	42.14	131.02	300.22	612.34
$M(3)$	15.57	54.17	168.64	386.38	787.01
$M(4)$	16.44	58.22	182.91	421.44	861.60
$M(5)$	17.05	60.77	192.69	446.70	917.27
Ratio	$E(1\rightarrow2)$	$E(2\rightarrow3)$	$E(3\rightarrow4)$	$E(4\rightarrow5)$	
$M(1)$	3.38	3.07	2.28	2.03	
$M(2)$	3.46	3.11	2.29	2.04	
$M(3)$	3.48	3.11	2.29	2.04	
$M(4)$	3.54	3.14	2.30	2.04	
$M(5)$	3.56	3.17	2.32	2.05	
Ratio	$E(1)$	$E(2)$	$E(3)$	$E(4)$	$E(5)$
$M(1\rightarrow2)$	1.57	1.61	1.63	1.64	1.67
$M(2\rightarrow3)$	1.28	1.29	1.29	1.29	1.29
$M(3\rightarrow4)$	1.06	1.07	1.08	1.09	1.09
$M(4\rightarrow5)$	1.04	1.04	1.05	1.06	1.06

TABLE VIII. Energy level spacing between the four most important orbitals that dominate the β of push-pull polyenes $NH_2(C_2H_2)_nNO_2$.

n	ΔE_o	ΔE_g	ΔE_u
1	8.02	3.68	2.02
2	8.41	2.85	1.66
3	8.71	2.25	1.56
4	8.88	1.90	1.40
5	9.03	1.63	1.26

The effect of energy level spacing is easy to observe because the number of important states are limited. Level spacings between four most important orbitals, two occupied and two unoccupied, are listed for all molecules and labeled as ΔE_o (two occupied), ΔE_g (HOMO-LUMO gap), and ΔE_u (two unoccupied), as shown in Table VIII. Both ΔE_g and ΔE_u decrease with respect to the chain length. Although ΔE_o increases with respect to chain length, it saturates when $n > 3$, and also since its magnitude is largest among the three ΔE, it therefore has the smallest influence because these ΔE appear in the denominator. Basically, the picture remains similar to the particle in a box one addressed in the previous $AgGa(S_xSe_{1-x})_2$ case, which suggests that a longer molecule has smaller energy level spacing, making its SHG coefficient larger.

Table IX shows the partial contribution to β from different parts of the push-pull polyenes, analyzed using atom-cutting approach.[28] It indicates that $(C_2H_2)_n$ units play a much more significant role than NO_2 and NH_2 end groups. Only for the shortest molecule does the NO_2 group become important. This decomposition of the sources of β into two end groups and conjugated chain segments allows one to understand the mechanism from a different viewpoint in addition to the band-resolving one.

IV. CONCLUSION

The plane wave pseudopotential DFT approach is adequate for present case studies. The sum-over-states formalism allows one to explicitly decompose SHG coefficients to more fundamental physical quantities such as energy levels and momentum matrix elements. This makes our band-resolved SHG analysis possible. Re-evaluation of SHG coefficients for crystals and molecules provides detailed information on the contribution to the SHG coefficient from a given subsystem or mechanism, which is either through partial band-index summation or through real-space wave functions partitioning, or even through the manipulation of energy levels.

Both the trend and the value of $\chi^{(2)}$ can be predicted for the anion substitution in $AgGa(S_xSe_{1-x})_2$ crystals. We have computationally proved that it is the cell volume that affecting the energy level spacing which then directly determines the variation of $\chi^{(2)}$ in these crystals. The material design for the desired optimal properties can indeed be achieved by controlling the substitution ratio.

TABLE IX. Partial contribution to β (in 10^{-30} esu) from the conjugate chain and end groups, their ratios to the total sum are given as the percentages in the parentheses. The original β of the whole molecules are also given in the last column, with the additivity error given in the square brackets.

n	NH_2	$(C_2H_2)_n$	NO_2	$H_2N(C_2H_2)_nNO_2$
1	0.14 (2%)	3.47 (48%)	3.55 (50%)	7.74 [7%]
2	4.12 (9%)	28.74 (62%)	13.63 (29%)	42.14 [10%]
3	22.92 (11%)	133.71 (67%)	43.15 (22%)	168.64 [18%]
4	63.85 (12%)	326.63 (69%)	98.33 (19%)	421.44 [24%]
5	202.92 (17%)	829.73 (70%)	150.45 (13%)	917.27 [29%]

In the case of nitroaniline molecules, VH contribution does not change much among the three structural isomers. This is not the case in the VE process, which is very large in *p*NA, drops significantly in *m*NA, and is very small with a cancellation effect in *o*NA. With the SHG-MO identified using band-resolved analysis, easy re-evaluation of β and making comparisons among the isomers are possible. It turns out that the trend of the SHG is determined by the matrix element part, which is indeed supposed to be sensitive to the change of orientation and bonding of push and pull functional groups on the plane of benzene ring.

As for the case of H_2N-$(C_2H_2)_n$-NO_2, the VE process dominates their hyperpolarizibility. Despite the fact that a longer molecule has very many more states than a shorter one, there is only an amazingly small number of the key $(\pi-)$ orbitals that contribute most to β. They are of the same characteristics and lying in the same order within energy level spectra. Re-evaluating β with adjusted energy levels of SHG-MO suggests that the trend of β is mainly determined by the energy level spectrum. Since a systematic decrease of energy level spacing with respect to the increase of chain length is observed, this explains why a longer push-pull polyene has a larger β. From the viewpoint of wave function partitioning, the hyperpolarzibility of these polyenes mainly comes from their conjugated chains, not their push and pull end groups.

In summary, the effects on SHG due to the size of unit cell, planar rearrangement of functional groups, and the length of conjugated chains are all investigated within the same framework of computation and analysis. We have demonstrated that the band-resolved (and wave function partitioning) SHG approach is a powerful tools to achieve better understanding to the mechanism of SHG of both crystals and molecules.

ACKNOWLEDGMENTS

The authors appreciate the useful discussion with Professor C. T. Chen in BCCRD and information provided by Dr. Chao-Ping Hsu in Academia Sinica. They are also grateful of NSC support of funding (NSC92-2112-M-032020) and the computing resources provided by NCHC.

[1] C. Aversa and J. E. Sipe, Phys. Rev. B **52**, 14636 (1995).
[2] E. Ghahramani, D. J. Moss, and J. E. Sipe, Phys. Rev. B **43**, 8990 (1991).
[3] A. G. Jackson, M. C. Ohmer, and S. R. LeClair, Infrared Phys. Technol. **38**, 233 (1997).
[4] V. Petrov, F. Rotermond, and F. Noack, J. Opt. A, Pure Appl. Opt. **3**, R1 (2001).
[5] S. N. Rashkeev and W. R. L. Lambrecht, Phys. Rev. B **63**, 165212 (2001).
[6] L. C. Tang, M.-H. Lee, C. H. Yang, J. Y. Huang, and C. S. Chang, J. Phys.: Condens. Matter **15**, 6043 (2003).
[7] M.-H. Lee and L.-C. Tang (unpublished).
[8] K. C. Rustagi and J. Ducuing, Opt. Commun. **10**, 258 (1974).
[9] M. Blanchard-Desce, I. Ledoux, J.-M. Lehn, J. Malthete, and J. Zyss, J. Chem. Soc., Chem. Commun., 237 (1988).
[10] M. Barzoukas, M. Blanchard-Desce, D. Josse, J.-M. Lehn, and J. Zyss, Chem. Phys. **133**, 323 (1989).
[11] M. Barzoukas, M. Blanchard-Desce, D. Josse, J.-M. Lehn, and J. Zyss, Inst. Phys. Conf. Ser. **103**, 239 (1989).
[12] R. A. Huijts and G. L. J. Hesselink, Chem. Phys. Lett. **156**, 209 (1989).
[13] H. Ikeda, Y. Kawabe, T. Sakai, and K. Kawasaki, Chem. Phys. Lett. **179**, 551 (1991).
[14] B. M. Pierce, in *Nonlinear Optical Organic Materials IV*, SPIE Proc. 1560 (SPIE, Bellingham, WA, 1991), p. 148.
[15] J. Messier, F. Kajzar, C. Sentein, M. Barzoukas, J. Zyss, M. Blanchard-Desce, and J.-M. Lehn, Nonlinear Opt. **2**, 53 (1992).
[16] C.-T. Chen and M.-H. Lee (private communication).
[17] T. Brotin, C. Ansraud, I. Ledoux, S. Brasselet, J. Zyss, M. Perrin, A. Thzet, and A. Collet, Chem. Mater. **8**, 890 (1996).
[18] H.-S. Kim, M.-H. Cho, and S.-J. Jeon, J. Chem. Phys. **107**, 1936 (1997).
[19] G. U. Bublitz, R. Ortiz, C. Runser, A. Fort, M. Barzoukas, S. R. Marder, and S. G. Boxer, J. Am. Chem. Soc. **119**, 2311 (1997).
[20] D. Jacquemin, B. Champagne, E. A. Perpete, J. M. Luis, and B. Kirtman, J. Phys. Chem. A **105**, 9748 (2001).
[21] M.-H. Cho, J. Phys. Chem. A **102**, 703 (1998).
[22] W. H. Thompson, M. Blanchard-Desce, V. Alain, J. Muller, A. Fort, M. Barzoukas, and J. T. Hynes, J. Phys. Chem. A **103**, 3766 (1999).
[23] P. Plaza, D. Laage, M. M. Martin, V. Alain, M. Blanchard-Desce, W. H. Thompson, and J. T. Hynes, J. Phys. Chem. A **104**, 2396 (2000).
[24] J. Abe, Y. Shirai, N. Nemoto, and Y. Nagase, J. Phys. Chem. A **101**, 1 (1997).
[25] M. C. Payne, M. P. Teter, D. C. Allan, T. A. Arias, and J. D. Joannopoulos, Rev. Mod. Phys. **64**, 1045 (1992).
[26] M.-H. Lee, Ph.D. thesis, University of Cambridge, 1995.
[27] S. N. Rashkeev, W. R. L. Lamberecht, and B. Segall, Phys. Rev. B **57**, 3905 (1998).
[28] J. Lin, M.-H. Lee, Z.-P. Liu, C. T. Chen, and C. J. Pickard, Phys. Rev. B **60**, 13380 (1999).
[29] Z. S. Lin, J. Lin, Z. Z. Wang, C. T. Chen, and M.-H. Lee, Phys. Rev. B **62**, 1757 (2000).
[30] Z. S. Lin, Z. Z. Wang, C. T. Chen, and M.-H. Lee, J. Appl. Phys. **90**, 5585 (2001).
[31] Z. S. Lin, Z. H. Wang, H. T. Yang, C. T. Chen, and M.-H. Lee, J. Chem. Phys. **117**, 2809 (2002).
[32] J. L. Oudar and D. S. Chemia, J. Chem. Phys. **66**, 2664 (1977).
[33] B. F. Levine, Chem. Phys. Lett. **37**, 516 (1976).
[34] L.-T. Cheng, W. Tam, S. H. Stevenson, G. R. Meredith, G. R. Rikken, and S. R. Marder, J. Phys. Chem. **95**, 10631 (1991).
[35] B. Champagne, E. A. Perpete, S. J. A. van Gisbergen, E.-J. Baerends, J. G. Snijders, C. Soubra-Ghaoui, K. A. Robins, and B. Kirtman, J. Chem. Phys. **109**, 15 (1998).
[36] J. P. Perdew, J. A. Chevary, S. H. Vosko, K. A. Jackson, M. Pederson, D. J. Singh, and C. Fiolhais, Phys. Rev. B **46**, 6671 (1992).